EINDHOVEN UNIVERSITY OF TECHNOLOGY

Department of Applied Physics
Crowdflow Research Group

The Hubbard Model in Crowd Dynamics

Bachelor Final Project

A.J. Hasenack

Supervisors:
prof. dr. F. Toschi
prof. dr. R. A. Duine

R-2121-SB

Eindhoven, June 2022

Abstract

In the relatively novel field of crowd dynamics, well established physical models may play an important role in explaining and predicting pedestrian behaviour. For example, force models and cellular automata have already been widely used. This raises the question on whether we can utilise methods from other fields of physics, too. If people are considered as Fermions – experiencing a repulsion which does not let two identical instances occupy a single position – the Bose-Hubbard model from condensed matter theory is not too far a stretch. In this model, the preferred positions depend on where people want to stay, how many people there are at one place and how willing people are to move across the region of interest. The underlying quantum mechanical framework (the so called second quantization) will first be studied in detail and solved for a two dimensional system. Then, the parameters in the model will be tuned in such a way that the model starts to represent groups of boarding people at train stations in the Netherlands. The idea of a Mott phase transition in the crowd is studied and successfully yields a critical density, $\rho_c \approx 0.22$ m^{-2}, above which pedestrians flow through more easily. A simulation of the boarding process is finally made after which the applicability of the model to crowd flow is discussed.

Preface

I wish to spend a few words here to thank my primary supervisor, Prof. dr. Federico Toschi for the stimulation of creative and critical thinking as well as for the opportunity to spend time on the specific topic of the second quantization in modern physics. He and the rest of the Crowdflow group were a great pleasure to work with. Moreover, I want to thank Prof. dr. Rembert Duine for the very useful, "ex machina"-like, help on specific theoretical problems.

Contents

Chapter 1

Introduction

Railway stations make up a large part of everyday public transport infrastructure. With over 1.3 million [6] travellers a day, the Netherlands has one of the busiest railways in Europe. Due to a combination of the pressing urge for climate change and the ever-growing population, crowd management is already and will be even more relevant in the future. Efficient use of pre-existing infrastructure and the calculation of whether new infrastructure can handle dense crowds are hence very valuable. Moreover, to ensure a safe, as well as efficient, passenger flow in railway stations, it is essential to unravel safety hazards and point out places of flow constriction. This requires new and innovative approaches capable of describing the expected data.

Various sub-fields of crowd dynamics can be identified. One can think of psychological behavioural models, in which mechanisms are explained by deducing how decision making processes in the brain work. Next to this, physical models can be used to make predictions about groups of people. This approach somewhat considers the psychological choices of the individual as a "black box", but captures relevant interactions with the environment. Examples of such interactions are obstacle avoidance or the repulsion pedestrians experience in order to move out of each others ways. A relatively straightforward method to model these interactions is via Newtonian force models [4]. If each object in one's surrounding is represented by a force (either attractive or repulsive) working at a certain distance and using the well-known "$F = m \cdot a$" relation, crowd trajectories can already be simulated. *Emergent phenomena* – a macro-scale phenomenon which arises from, but is not encoded in the traits of the individual – such as clogging at door entrances, zipping in queues and lane formation in opposing streams of people [3] can herewith be explained. In essence these physical models are not representing any truly existing forces. The beauty, however, lies in the ability of describing as much phenomena with as little parameters as possible. For that, often models are considered that stem from other disciplines in physics which may have some overlapping characteristic with the crowd. One such characteristic is the tendency of the individual to have a finite dimension and thus occupy a certain area on the floor. Especially in high-density situations this incompressibility-like trait plays an important role in understanding crowd-distribution. Hydrodynamical considerations, in which we regard a group of people as a fluid, can be used to yield occupation densities following the incompressibility condition

$$\vec{\nabla} \cdot \vec{v} = 0 \tag{1.1}$$

However, this requires us to accept the analogy of regarding one person as some sort of fluid parcel, as hydrodynamics is inherently continuous. A discrete description, which still captures the impossibility of stacking people on top of each other, regards the individuals as Fermions. A Fermion is one of two types of particles in nature, the other being a Boson, which is by definition characterised by the *Pauli-exclusion principle*: a mechanism in nature that ensures that no two Fermions which are in identical state (read: have similar energies, momenta, etc.) can occupy the same location in space. Bosons, on the other hand, are able to sit together with infinetely many instances. In figure 1.1 a 2D grid of which the boxes can be precisely occupied by one particle. The natural size for these boxes is the *De Broglie wavelength*, which can be seen as the size the

particles take up in space. Viewing pedestrians this way (that is, they cannot be at the same

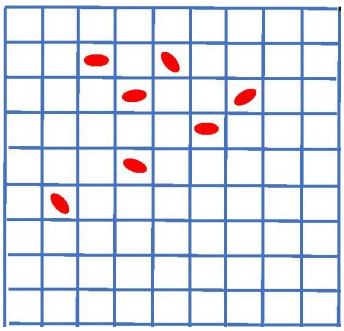

Figure 1.1: Illustration of the Pauli exclusion principle for pedestrians. Spots are only occupied by either zero or one (identical) particle.

time at the same position) leads us in an interesting direction. If a space-discretization is applied to a certain (for example two dimensional) region of interest exactly of the width and depth of a person, the "particles" we put on this grid can be said to experience a similar sort of exclusion. In this case, either zero or one particle fits in the box. It is, however, quite convenient in the case of crowd dynamics to have a slightly larger box size. This essentially violates the criterion for Pauli exclusion, but the idea remains the same. Unlike the case with Fermions, the cap on the number of passengers per lattice site will be set equal to N, the number of people that can maximally physically fit in a site of a given dimension. It is necessary to point out that thus the way we will view pedestrians will neither be as Fermions nor Bosons, but something in between, an intermediate description that is called *parastatistics*.

Now, it may be a possibility that one of these *sites* of the grid, is more preferable to stand on than the other. This is the case at a train platform; During the waiting for the train to arrive, coffee corners are common places to get drawn to. The sides of the platform however, carry an inherent repulsion-like characteristic, which makes them less occupied. Let us give a name to the repulsion of an arbitrary site ℓ: V_ℓ. If the repulsion is high, a person most likely would not prefer occupying the spot. If it is low on the other hand, he or she is drawn to it. This repulsive term describes in fact the psychological preferences of pedestrians, something which we cannot trivially extract. What can be done to overcome this problem, is to measure during a longer period of time where people typically like to walk and wait. Averaging these densities in time gives an estimate for the repulsion, which can then be used for modeling. However, just as the Fermions we just introduced, there is a cap on how many pedestrians can occupy the least repulsive places. If the spot is already quite full, it will most likely be the case that an incoming pedestrian will occupy a surrounding site with a slightly higher value of V_ℓ. This interaction that people experience can be modeled by introducing a second cost that needs to be paid to occupy site ℓ: $U(n_\ell - 1)$. This cost now scales with the number of people already present, n_ℓ, because the dissatisfaction will be very high if the site is overfull already. The currency that can be used to pay for these two repulsive interactions, is energy and it flows into the system in the form of a (typical) kinetic energy, J, and an energy term that each particle carries with them when flowing into the region of interest, μ. Even though in reality, the system of pedestrians walking on a platform does not conserve energy[1], the model can represent a subset of the pedestrians present, those with kinetic energy J. In figure 1.2 an illustration of a train platform can be found with the corresponding energy terms. The site dependent *potential*, V_ℓ, here has a trough close to the train door to stress the preference to board quickly, but a peak near to the edge of the platform due to the caution for falling on the tracks.

The possible pedestrian configurations arising from the potentials can in a static situation fully be described by the number of pedestrians per site, the *occupation numbers* g_ℓ. The goal of the

[1]The system can be viewed as a lattice full of *active matter*, where the particles can in fact propel themselves.

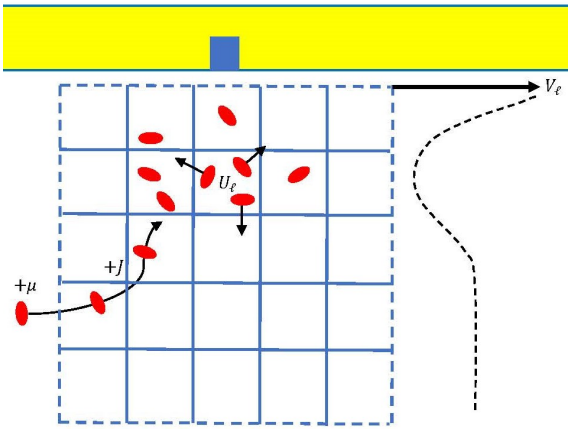

Figure 1.2: Illustration of the energy terms in the proposed model for the description of the crowd at a train station. The energy per person, μ, and kinetic energy, J, flow into the system and are used to occupy a spot with site dependent potential, V_ℓ, and interaction potential U.

following chapters is to find suitable potentials, V_ℓ, U, J and μ such that the occupation numbers that we predict are in accordance with what is measured at train stations in the Netherlands. The power of the proposed model, we will introduce shortly, lies not only in the configurations it can make predictions about, but it also has the ability to simulate the time evolution of the system in study. Moreover, the emergent phenomenon of a *phase transition* – from a phase in which groups of people block flow (the so called *insulator* phase) to a phase in which people are easily let through (the *superconductor* phase)– is inherent to the model. We expect that, to some extent, such a transition can be identified in the crowd. In the situation that there is a low density at a preferable spot, newly arriving passengers are likely to occupy it. The relatively empty spot, in essence, blocks flow due to attraction. If the preferable location is on the other hand already quite crowded, passengers are expected to continue walking, thus increasing the flow over the spot. It is postulated that there exists some value for the density at which such a transition must take place.

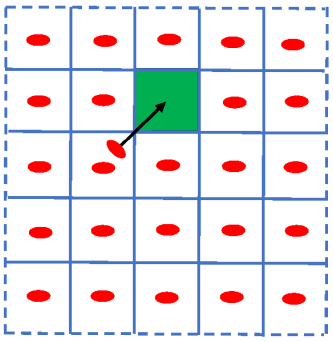

Figure 1.3: Illustration of the particle capture process in the insulator phase. Because the surrounding tiles all have a density higher than the empty green tile, the green tile blocks particle flow.

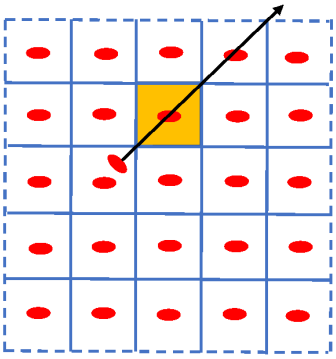

Figure 1.4: Illustration of the superfluid phase. The orange and surrounding tiles are not very attractive because they are already filled. The particle moves freely over the crowded tiles in search of lower densities.

In chapter 2, the relevant framework to study the mentioned configurations is formally set-up, after which a theoretical way to estimate the point of the phase transition is described. Then, solutions for the occupation numbers are found and time dynamics are incorporated into the solution. Chapter 3 is dedicated to applying the model to boarding processes at train stations and finding suitable parameters, yielding a simulation of the railway platform. Then, we continue by discussing the efficacy of the model in chapter 4 and give some space for reflection on possible points of improvement and options for the future.

Chapter 2

Theory

We now turn to a formal description of a discrete system of particles. A lattice is introduced of which the sites can be described by $\ell = (\ell_x, \ell_y)$. They are each occupied by g_ℓ particles with a certain velocity $\vec{v}_\ell$. In the following, a quantum mechanical description of the energy arising from the occupation numbers is derived. This framework is necessary to identify critical values of the potentials for the insulator - superfluid phase transition. Using the principle of energy minimization, a procedure to find the optimal configurations is sketched. Lastly, the influence of possible time dependency of the potentials is studied.

2.1 Second quantization

The field of quantum mechanics focuses on the quantization of certain parameters. An example of such a parameter is the energy of a state, of which the spectrum can be found by calculating the solutions to the Schrödinger equation for e.g. the harmonic oscillator. In practice we indeed find that measuring the energy will yield these discrete values. But we can go a step beyond observables like energy. The excitations in the particle fields (Bosonic and Fermionic) can themselves be quantized such that we can actually speak about a single particle, what is called the *second quantization*. For this, we have to define a framework which can extract the amount of particles from the known states (wave-functions) and can possibly add and subtract particles to the state. The *creation* and *annihilation operators* do exactly this. We distinguish different such operators for bosonic and fermionic systems but here, the focus will be laid upon bosons. The bosonic creation, $\hat{b}_\ell^\dagger$, and annihilation, $\hat{b}_\ell$, operators are fully defined by their commutation relations

$$[\hat{b}_\ell, \hat{b}_m^\dagger] = \delta_{\ell m}\hat{1} \tag{2.1}$$

where the indices refer to discretized loci in space, for example on a lattice. The operators work on vectors in the so-called *Fock space*. The construction of this space starts by considering the single-particle bosonic Hilbert spaces on lattice sites ℓ, $\{\boldsymbol{H}_\ell\}$. Then, the Fock space is defined by the direct sum over symmetric product of all possible site-occupancy combinations

$$\boldsymbol{\mathcal{F}} = \bigoplus_{N=1}^{\infty} \bigvee_{\ell=1}^{L} \boldsymbol{H}_\ell^{n_\ell \vee} \tag{2.2}$$

where $\boldsymbol{H}_\ell^{n_\ell \vee}$ is the symmetric product of n_ℓ particles on each lattice site such that $\sum_{\ell=1}^{L} n_\ell = N$. Each state in the Fock space $\boldsymbol{\mathcal{F}}$ is denoted by $|n_1 \ \dots \ n_L\rangle$. A suitable basis for this space is the infinite *occupation number basis*

$$\{|k_\ell\rangle \equiv |0 \ \dots \ k_\ell \ \dots \ 0\rangle \ \big| \ k_\ell = 0, 1, 2, \dots \ , \ \ell = 1, \dots, L\} \tag{2.3}$$

for which we have the orthogonality relations

$$\begin{cases} \langle k_\ell | k_m \rangle = 0 & \ell \neq m \\ \langle k_\ell | l_\ell \rangle = 0 & k \neq l \end{cases} \tag{2.4}$$

Properties of this basis are completeness and no normalization. The effect of the creation and annihilation operators on a general state then is

$$\begin{cases} \hat{b}_\ell^\dagger \, |n_1 \ \dots \ n_L\rangle = \sqrt{n_\ell + 1} \, |n_1 \ \dots \ n_\ell + 1 \ \dots \ n_L\rangle \\ \hat{b}_\ell \, |n_1 \ \dots \ n_L\rangle = \sqrt{n_\ell} \, |n_1 \ \dots \ n_\ell - 1 \ \dots \ n_L\rangle \end{cases} \tag{2.5}$$

The *number operator* is defined as $\hat{n}_\ell = \hat{b}_\ell^\dagger \hat{b}_\ell$ and its purpose is to extract the number of particles in a certain state. It is straightforward to see that every vector in the Fock space is an eigen-vector of the number operator and indeed it extracts the number of bosons

$$\hat{n}_\ell \, |n_1 \ \dots \ n_L\rangle = n_\ell \, |n_1 \ \dots \ n_L\rangle \tag{2.6}$$

In this formalism of the occupation number basis, the effect of the previously mentioned operators can also be expressed in matrix form. In order to do so however, we cannot escape from setting an upper-bound to the maximum of particles per lattice site. Denote it by M for now. The occupation number basis is now finite and we can make a $M^L \times M^L$ matrix for the creation and annihilation operators

$$\begin{aligned} \hat{b}_\ell^\dagger &= \hat{1}_1 \otimes \cdots \otimes \hat{1}_{\ell-1} \otimes \begin{pmatrix} 0 & 0 & 0 & 0 & \dots \\ \sqrt{1} & 0 & 0 & 0 & \dots \\ 0 & \sqrt{2} & 0 & 0 & \dots \\ 0 & 0 & \sqrt{3} & 0 & \dots \\ \vdots & \vdots & \vdots & \vdots & \ddots \end{pmatrix} \otimes \hat{1}_{\ell+1} \otimes \cdots \otimes \hat{1}_L \\ \hat{b}_\ell &= \hat{1}_1 \otimes \cdots \otimes \hat{1}_{\ell-1} \otimes \begin{pmatrix} 0 & \sqrt{1} & 0 & 0 & \dots \\ 0 & 0 & \sqrt{2} & 0 & \dots \\ 0 & 0 & 0 & \sqrt{3} & \dots \\ 0 & 0 & 0 & 0 & \dots \\ \vdots & \vdots & \vdots & \vdots & \ddots \end{pmatrix} \otimes \hat{1}_{\ell+1} \otimes \cdots \otimes \hat{1}_L \end{aligned} \tag{2.7}$$

These operators are used in the following model.

2.2 The Bose - Hubbard model

Now the framework of the Fock space is introduced, a model for the behaviour of the system can be defined. It is expected that crowds will be experiencing a few fundamental forces. The first one being the attractiveness of certain places. Train doors, escalators and benches are examples of these. Secondly, mutual passenger interactions cause that no spot can be crowded more than a certain amount. Hence, a cost scaling with the square of the number of passengers seems a logical choice. Then, there is the effect of moving over the platform. Considering that passengers carry kinetic energy, it is not unlikely that the pedestrians will not exactly end up at the most desirable spot, but in the neighbourhood of it. A model that fulfills all of these criteria, is the so called Bose - Hubbard model from condensed matter physics. This is a form of a Hubbard model which typically accounts for Bosons instead of Fermions. However, since we study a repulsive interaction potential (which for Bosons would be attractive), the particles in question will behave quasi-Fermionic. The Bose - Hubbard model is used to study superfluid - Mott insulator phase transitions [8]. These Mott insulator states are particular to the Hubbard model, and could not be determined with regular band theory. The model is applied to e.g. optical lattices and has

applications in quantum computing [5]. The three previously described forces are represented by the potential terms V_ℓ, U and J (see equation 2.8). Additionally, a term covering the chemical potential, μ, is present, such that we can study the statistics of the system in the grand-canonical ensemble. Herein, particles can freely flow out of and into the lattice, taking their energy (the chemical potential) with them. The Bose - Hubbard model is based around the Hamiltonian operator

$$\hat{\mathcal{H}} = -J \sum_{\langle \ell, m \rangle} \hat{b}_\ell^\dagger \hat{b}_m + \frac{1}{2} U \sum_\ell \hat{n}_\ell (\hat{n}_\ell - 1) + \sum_\ell V_\ell \hat{n}_\ell - \mu \sum_\ell \hat{n}_\ell \tag{2.8}$$

of which the eigenstates, $\{|\psi\rangle\}$, satisfy the time independent Schrödinger equation

$$\hat{\mathcal{H}}|\psi\rangle = E|\psi\rangle \tag{2.9}$$

The meaning of the first term in 2.8 is the creation of a particle at site ℓ and destruction at m according to a cost of $-J$. The notation $\langle \ell, m \rangle$ means that only nearest neighbours are considered. For one dimension we have two nearest neighbours, for two dimensions four and three dimensions six. The other terms extract the number of particles and multiply this with the previously mentioned potential terms.

2.3 Kinetic free case

It is generally not possible to immediately derive the eigenstates of the Bose-Hubbard Hamiltonian. That is why first some more basic cases need to be studied. Already quite some behaviour can be predicted by neglecting the kinetic energy term, thus setting $J = 0$. Define the zero-kinetic energy Hamiltonian as

$$\hat{\mathcal{H}}_0 = \frac{1}{2} U \sum_\ell \hat{n}_\ell (\hat{n}_\ell - 1) + \sum_\ell V_\ell \hat{n}_\ell - \mu \sum_\ell \hat{n}_\ell \tag{2.10}$$

This can also be written in continuous form. To do so, the discrete site occupation numbers (n_ℓ) are replaced with the density, $n(\boldsymbol{x})$, mirroring the approach in Density Functional Theory [1]. This makes that the Hamiltonian changes accordingly as

$$\hat{\mathcal{H}}_0[\hat{n}] = \frac{1}{2} U \int d\boldsymbol{x}\ \hat{n}(\boldsymbol{x})(\hat{n}(\boldsymbol{x}) - 1) + \int d\boldsymbol{x}\ (V(\boldsymbol{x}) - \mu)\hat{n}(\boldsymbol{x}) \tag{2.11}$$

and applied to a state

$$E^{(0)}[n] = \frac{1}{2} U \int n(\boldsymbol{x})(n(\boldsymbol{x}) - 1) d\boldsymbol{x} + \int (V(\boldsymbol{x}) - \mu) n(\boldsymbol{x}) d\boldsymbol{x} \tag{2.12}$$

Taking the functional derivative with respect to the ground state density, $n(\boldsymbol{x})$, we get that

$$\frac{\delta E^{(0)}[n]}{\delta n} = 0 \Rightarrow g^{(0)}(\boldsymbol{x}) \equiv \frac{\mu - V(\boldsymbol{x})}{U} + \frac{1}{2} \tag{2.13}$$

Leaving us with

$$E^{(0)}[g^{(0)}] = -\frac{1}{2} U \int \left(g^{(0)}(\boldsymbol{x}) \right)^2 d\boldsymbol{x} \tag{2.14}$$

Discretizing again yields

$$g_\ell^{(0)} = \frac{\mu - V_\ell}{U} + \frac{1}{2} \tag{2.15}$$

and for $g_\ell = g_\ell^{(0)}$

$$E^{(0)}(g_\ell^{(0)}) = \sum_{\ell=1}^{L} E_\ell^{(0)}(g_\ell^{(0)}) = -\frac{1}{2} U \sum_{\ell=1}^{L} (g_\ell^{(0)})^2 \tag{2.16}$$

with L now explicitly the number of sites. As a consistency check, it can be found that indeed

$$g_\ell^{(0)} = -\frac{\partial E_\ell^{(0)}(g_\ell^{(0)})}{\partial \mu} \tag{2.17}$$

Example 2.3.1. Until now, we have seen a way to theoretically describe the energies of configurations. It is interesting to see whether already some numerical solutions for the ground state can be compared with the theory. Moreover, solving the Hamiltonian numerically puts us in the position to also consider cases for $J > 0$, something which we cannot do yet analytically. We turn to a simple case study of a 1D chain of length L subject to a harmonic potential

$$V_\ell = \left(\ell - \frac{L-1}{2}\right)^2 \tag{2.18}$$

and $U = 1$, $\mu = 3.5$. The way to solve the Bose - Hubbard model for these potentials is to fix an upper bound for the number of particles per lattice site, like we demonstrated in 2.1. Let us take $M = 5$ for now. Then, the creation and annihilation operators from equation 2.7 are combined to make a $M^L \times M^L$ matrix representation for the Bose - Hubbard model. On the diagonals of this matrix, the energy contribution is only associated to single latice sites. On the off-diagonals, however, nearest neighbour interactions arising from the kinetic energy make up additional energy contributions. In the occupation number basis (see 2.3), each state in the Fock space is a superposition of the possible occupation number configurations. The probability amplitudes of these states can be put inside a vector of length M^L. The (time independent) Schrödinger equation now is a relatively straightforward matrix eigenvalue problem

$$(\underline{\mathbf{H}} - E)\boldsymbol{\psi} = 0 \tag{2.19}$$

where $\underline{\mathbf{H}} \in \mathbb{C}^{M^L} \times \mathbb{C}^{M^L}$, $E \in \mathbb{R}$ and $\boldsymbol{\psi} \in \mathbb{C}^{M^L}$. Multiple eigenvalues can be found. Of all these, the ground state is given by the state with the lowest eigenenergy. Given the fact that the probability amplitudes correspond to the occupation number configurations of all the lattice sites combined, we cannot represent single site probability amplitudes. What can be done however, is to calculate the unconditional probability of finding g_ℓ particles on lattice site ℓ by integrating over the probability of each state in the Fock space which has g_ℓ particles on lattice site ℓ.

$$\mathbb{P}(g_\ell \text{ particles on } \ell) = \int \cdots \int_0^M \mathbb{P}(|n_0 \dots g_\ell \dots n_L\rangle)\, dn_0 \dots dn_L \tag{2.20}$$

Using this procedure a graphical representation can be constructed. We first solve the system for $J = 10^{-5} \approx 0$, corresponding to the kinetic free case, which can be seen in the figure 2.1. The theoretical prediction for the occupation numbers is added in blue, corresponding very well with the numerical solution. When the kinetic energy is turned on, $J = 0.5$, it can be seen in figure 2.2 that a sort of smearing of the probability amplitude occurs. This makes sense, because the states just next to the most favorable ones are now accessible too, due to additional kinetic energy. The goal in the sections below is to also be able to make theoretical predictions about the case with $J > 0$.

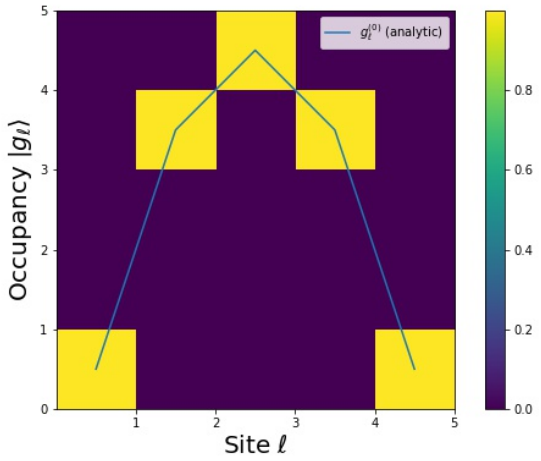

Figure 2.1: Numerical solution and theoretical prediction for the unconditional probability amplitudes of the occupation numbers for the kinetic free Bose-Hubbard model on a 1D chain with a harmonic potential.

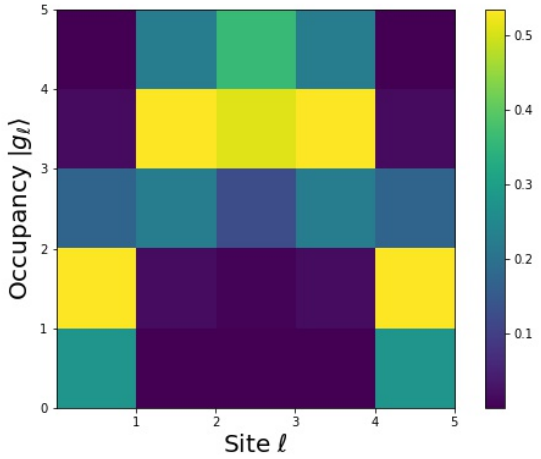

Figure 2.2: Numerical solution for the unconditional probability amplitudes of the occupation numbers for the Bose-Hubbard model on a 1D chain with a harmonic potential.

2.4 Mean field theory

Consider now the contribution of hopping between sites due to kinetic energy

$$\hat{\mathcal{H}}_h = -J \sum_{\langle \ell, m \rangle} \hat{b}_\ell^\dagger \hat{b}_m \tag{2.21}$$

Because of this term, it is not possible to write the total Hamiltonian as sum over the single sites. This means that nearest neighbours are inevitably entangled and we cannot write the total wavefunction as a tensor product of the single site wavefunctions

$$|n_1\ n_2\ \ldots\ n_L\rangle \neq |n_1\rangle \otimes |n_2\rangle \otimes \cdots \otimes |n_L\rangle \tag{2.22}$$

where we have denoted $|n_\ell\rangle$ for the wavefunction on site ℓ with n_ℓ particles. Computationally, this proves to be a problem, as solving the system for the entangled Hamiltonian involves calculating eigenvalues of a matrix that scales with the power of the number of lattice sites. If the system obeys translation symmetry ($U_i = \text{const.}$ and $V_i = \text{const.}$) or particle number conservation ($\mu = 0$), it would be possible to split the full Hamiltonian into domains [7], but no such tricks can be evoked for our particular case. That is why a mean field (or decoupling) approach is used. Let us introduce the (discrete) order field as in [9]

$$\psi_\ell = \langle \hat{b}_\ell^\dagger \rangle = \langle \hat{b}_\ell \rangle = \sqrt{n_\ell} \tag{2.23}$$

We then let the creation and annihilation operators act like a perturbation on the mean field such that

$$\begin{cases} \hat{b}_\ell^\dagger \mapsto \psi_\ell + \hat{b}_\ell^\dagger \\ \hat{b}_\ell \mapsto \psi_\ell + \hat{b}_\ell \end{cases} \tag{2.24}$$

where it is assumed that $\psi_\ell \in \mathbb{R}$. Considering that for this perturbation $\langle \hat{b}_\ell^\dagger \hat{b}_m \rangle \ll \langle \psi_\ell \hat{b}_m \rangle$, we get that the hopping term of the Hamiltonian can be expressed as

$$\hat{\mathcal{H}}_h \approx -J \sum_{\langle \ell, m \rangle} \left(\psi_\ell \psi_m + \psi_m \hat{b}_\ell^\dagger + \psi_\ell \hat{b}_m \right) \tag{2.25}$$

Using the symmetry properties of $\langle \ell, m \rangle$ and using $\psi_m \approx \psi_\ell$ for all z nearest neighbour pairs, after simplification we get

$$\hat{\mathcal{H}}_h \approx -Jz \sum_\ell \psi_\ell (\psi_\ell + \hat{b}_\ell^\dagger + \hat{b}_\ell) \tag{2.26}$$

which yields the desired independence of the lattice sites

$$\hat{\mathcal{H}}_{\mathcal{MF}} = \sum_\ell \hat{\mathcal{H}}_\ell \tag{2.27}$$

with

$$\hat{\mathcal{H}}_\ell = -Jz\psi_\ell(\psi_\ell + \hat{b}_\ell^\dagger + \hat{b}_\ell) + U\hat{n}_\ell(\hat{n}_\ell - 1) + (V_\ell - \mu)\hat{n}_\ell \tag{2.28}$$

This decoupling of the Hamiltonian already allows us to calculate some interesting aspects of the Hubbard model.

2.5 Mott-transition

It is expected that for certain values of the potentials, the system of Bosons act differently then others. If there is a large kinetic energy for example, the particles are free to move as much as they want. While if the kinetic energy is small, the particles are confined to the most favorable states. To calculate the transition point, we take a Landau approach. It will turn out that we will find a boundary between the Mott-insulator and the superfluid phase.

We start off by introducing perturbation theory in orders of ψ_ℓ. Looking at the effect of the hopping perturbation to the kinetic free Hamiltonian, we see that the odd order energy corrections are zero, leaving us with the even ones. It can hence be posed that the total ground state energy to second order in ψ_ℓ can be written as

$$E_\ell = E_\ell^{(0)} + E_\ell^{(2)} + \cdots = a_0 + a_2\psi_\ell^2 + \mathcal{O}(\psi_\ell^4) \tag{2.29}$$

The second order energy correction is calculated using

$$E_\ell^{(2)} = \sum_{m \neq g_\ell} \frac{\left| \langle m_\ell | \ \hat{\mathcal{H}}_h \ | g_\ell \rangle \right|^2}{E_\ell^{(0)}(g_\ell) - E_\ell^{(0)}(m_\ell)} \tag{2.30}$$

and since for each site $\langle m|n\rangle = \delta_{mn}$, we find that

$$E_\ell^{(2)}(g_\ell) = -Jz\psi_\ell^2 - \left(\frac{g_\ell^{(0)} - \frac{1}{2}}{(g_\ell - g_\ell^{(0)})^2 - \frac{1}{4}}\right)\frac{(Jz)^2}{U}\psi_\ell^2 \tag{2.31}$$

Considering that E_ℓ should be minimal, the following two cases hold for some minimizing order parameter, $\psi_{\ell,\min}$

$$\begin{cases} a_2 > 0 \Rightarrow \psi_{\ell,\min} = 0 \\ a_2 < 0 \Rightarrow \psi_{\ell,\min} \neq 0 \end{cases} \tag{2.32}$$

Then at $a_2 = 0$ there must be a boundary between two phases, here a superfluid and insulator phase. If we solve this condition for μ, two branches can be found

$$\frac{\mu_\pm - V_\ell}{U} = 2\left(g_\ell - \frac{1}{2}\right) - \frac{Jz \pm \sqrt{Jz\left(Jz - 4(g_\ell - \frac{1}{2})U\right) + U^2}}{2U} \tag{2.33}$$

An example of a phase diagram can be found in figure 2.3. The general shape of the diagram is in agreement with the literature [2], with understandably an extra contribution from the potential, V_ℓ. In the encapsulated region we speak about an insulator phase, while on the right side, where there is enough kinetic energy (J) to freely hop, the particles behave as a superfluid. It can

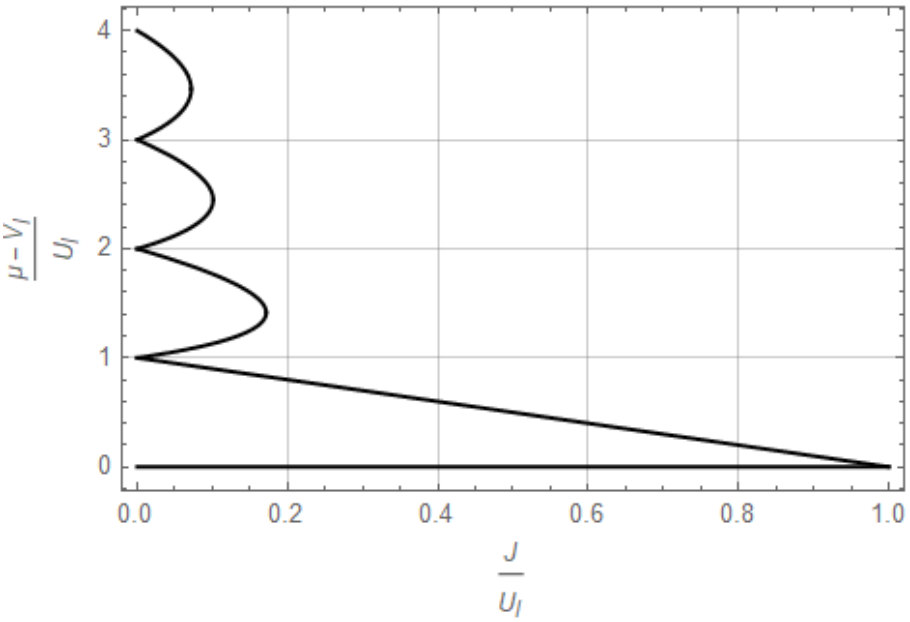

Figure 2.3: Example Mott phase transition diagram for $V_\ell = U = 1$ and $g_\ell = 1, 2, 3, 4$.

moreover be seen that the transition line crosses the vertical axis at integer values. This is due to the fact that once a set of lattice sites is exactly filled with g_ℓ particles, i.e.

$$\mu = g_\ell U + V_\ell \tag{2.34}$$

the next particle has no preferred location to go to. It will freely move across the lattice and thus behave as a superfluid, too. Last of all, we can find a critical hopping potential, J_c, by equating the positive and negative branch of 2.33.

$$\frac{J_c}{U} = \left(g_\ell - 2 + 2\sqrt{(g_\ell - 1)g_\ell}\right) \tag{2.35}$$

signifying the peaks in the above figure.

2.6 Self-consistency

The single site Hamiltonian of equation 2.28 can be diagonalized in order to find its eigenfunctions, $\{|\phi_\ell\rangle_i\}$, and eigenenergies, $\{E_{\ell,i}\}$. The smallest eigenenergy determines the single site ground state, denote it by $|\phi_\ell\rangle$. On the premise that the latter poses a self-consistent mean field theory, it can be stated that

$$\psi_\ell = \langle\phi_\ell|\hat{b}_\ell|\phi_\ell\rangle \tag{2.36}$$

Because the functions $|\phi_\ell\rangle$ depend on ψ_ℓ, no analytic result can be derived this way. However, it is possible – under the assumption that the map described in the following is contracting – to iteratively converge to the true values for $|\phi_\ell\rangle$, ψ_ℓ. In 1, a method is described to calculate the occupation numbers for each lattice site ℓ. This algorithm now scales linearly with the number of sites and thus can cope with higher particle and lattice site numbers than the full diagonalization.

Algorithm 1 Iterative self-consistent mean field

Choose $|\phi_\ell\rangle^{(0)}$ non-zero
while $i \leq$ iterations **do**
Calculate the next order parameter

$$\psi_\ell^{(i)} \equiv \langle\phi_\ell^{(i-1)}|\hat{b}_\ell|\phi_\ell^{(i-1)}\rangle$$

Find the next set of eigenstates

$$\{|\phi_\ell\rangle_j^{(i)}\}, \{E_{\ell,j}^{(i)}\}$$

Find state with smallest energy

$$k = \underset{j\in\mathbb{N}}{\arg\min}\left(E_{\ell,j}^{(i)}\right), |\phi_\ell^{(i)}\rangle \equiv |\phi_\ell^{(i)}\rangle_k$$

end while
Calculate $g_\ell \equiv \langle\phi_\ell^{(\text{iterations})}|\hat{b}_\ell^\dagger\hat{b}_\ell|\phi_\ell^{(\text{iterations})}\rangle$

One artifact of the proposed mean field theory is ignoring the particle number conservation. This causes that for an increasing hopping potential, J, generally not only the shape of the lattice site occupation, but also the total number of particles changes. To account for this, the mean number of particles per lattice site of the $J = 0$ case is matched with the $J > 0$ case such that

$$\tilde{g}_\ell = g_\ell + \frac{1}{L}\sum_{m=1}^{L}\left(g_m^{(0)} - g_m\right) \tag{2.37}$$

in which $g_m^{(0)}$ is the set of occupation numbers in 2.15. This forces the sum of particles to be the same in both cases.

2.7 Dynamics

Now that a static description is found, the next step is to incorporate time dependent perturbations to the Hamiltonian. For this, it is quite useful to change from the traditional Schrödinger picture, to the more suitable *interaction picture* to describe both state vectors and operators. The interaction picture can be seen as an intermediate step between the Schrödinger – in which states carry time dependence – and the Heisenberg picture – in which observables carry time dependence. Consider first the regular solution to the Schrödinger equation for a time independent Hamiltonian

$$|\psi(t)\rangle = \hat{U}(t)\ |\psi(0)\rangle \tag{2.38}$$

where

$$\hat{U}(t) = e^{-i\hat{\mathcal{H}}_0 t} \tag{2.39}$$

is the unitary time evolution operator (for $\hbar = 1$), which should not be confused with the interaction potential from the latter. The interaction picture, now, makes use of the premise that the time dependent Hamiltonian can be written as

$$\hat{\mathcal{H}}(t) = \hat{\mathcal{H}}_0 + \hat{\mathcal{H}}'(t) \tag{2.40}$$

for which $\hat{\mathcal{H}}'(t)$ is assumed to be relatively small. We then continue by introducing the interaction picture transformations for a general set of state vectors and observables

$$\begin{cases} |\psi_I(t)\rangle = \hat{U}^\dagger(t)\ |\psi(t)\rangle \\ \hat{A}_I(t) = \hat{U}^\dagger(t)\ \hat{A}(t)\ \hat{U}(t) \end{cases} \tag{2.41}$$

If then the interaction picture equivalent of the Hamiltonian is inserted in the Schrödinger equation, we see by invoking the unitary property and the self-commuting property, $[\hat{\mathcal{H}}_0, \hat{U}(t)] = 0$, that

$$\begin{aligned} i\partial_t\ \hat{U}(t)\ |\psi_I(t)\rangle =&\ \hat{U}(t)\ \hat{\mathcal{H}}(t)\ \hat{U}^\dagger(t)\ \hat{U}(t)\ |\psi_I(t)\rangle \\ \iff \hat{U}(t)\ i\partial_t\ |\psi_I(t)\rangle + \hat{U}(t)\ \hat{\mathcal{H}}_0\ |\psi_I(t)\rangle =&\ \hat{U}(t)\ \left(\hat{\mathcal{H}}_0 + \hat{\mathcal{H}}'(t)\right)\ |\psi_I(t)\rangle \\ \iff i\partial_t\ |\psi_I(t)\rangle =&\ \hat{\mathcal{H}}'(t)\ |\psi_I(t)\rangle \end{aligned} \tag{2.42}$$

The solution to this alternative Schrödinger equation is given in terms of the Dyson series

$$|\psi_I(t)\rangle = \hat{T} \exp\left(-i \int_0^t d\tau\ \hat{\mathcal{H}}'(\tau)\right) |\psi_I(0)\rangle \tag{2.43}$$

with $\hat{T}$ the time-ordering operator. To first order we thus have

$$|\psi_I(t)\rangle \approx \left(1 - i \int_0^t d\tau\ \hat{\mathcal{H}}'(\tau)\right) |\psi(0)\rangle \tag{2.44}$$

where we have used $|\psi_I(0)\rangle = |\psi(0)\rangle$. After this, the interaction picture solution can be transformed back to the Schrödinger picture which makes that the occupation numbers can again be calculated. For the single site Hamiltonian and wave-functions of section 2.4 this yields

$$g_\ell(t) = \left\langle \hat{U}_\ell(t)\ \phi_{I,\ell}(t) \ \middle|\ \hat{n}_\ell\ \hat{U}_\ell(t)\ \phi_{I,\ell}(t) \right\rangle \tag{2.45}$$

where $\hat{U}_\ell = e^{-i\hat{\mathcal{H}}_\ell t}$ and $|\phi_{I,\ell}(t)\rangle$ is found using equation 2.44 with $\hat{\mathcal{H}}'_\ell(t)$ as a yet to be specified perturbation.

Chapter 3

Results & Conclusion

Since the theoretical framework for the Bose - Hubbard model is discussed, we can now consider its application into crowd dynamics. For this, we need to match the potentials (V_ℓ, U, μ and J) to the available data. The data that will be studied are time and position points of pedestrians at train stations in the Netherlands (mainly at Eindhoven Central station). The space dependent potential, V_ℓ, will be determined at the moment of a boarding train, during which a crowd forms near the train doors. Moreover, the point of a phase transition will be derived from the whole platform, at which we will study still standing - moving passenger interactions. Finally, the potential, V_ℓ, is modulated in time, such that the dynamics can be obtained.

3.1 Train boarding potential

In order to find an expression for the potential, V_ℓ, during the boarding process, a data set consisting roughly of 3000 events is considered. Every event is a collection of trajectories of a few minutes in which people first align to board, and then board. For this, we observe various train doors. Each of these events is first split up into 20 fragments. Then, boolean masks are applied on the fragments, filtering unique people on the following criteria, in consecutive steps

1. Only in the region of interest ($w \times h = 12 \times 2$ m^2, with the train door in the horizontal middle, vertical top)
2. Sufficiently low vertical velocities, such that moments of active boarding are disregarded ($|v_y| < 0.1$ m/s)

Then the busiest moment is identified, which now only takes into account waiting people. Then bins are created in the horizontal and vertical directions of size $\Delta x \times \Delta x = 0.1 \times 0.1$ m^2. Considering that the width of human shoulders is approximately $\Delta w \approx 40$ cm an upper bound for the occupation numbers per site is yielded: $N_{\max} = \Delta x^2/\Delta w^2 = 6.25 \cdot 10^{-2}$. But this will most likely not be achievable, as people try to keep their distance even during boarding. Now, the number of people per state per bin can be collected and we average over all the events, yielding the 2D occupation numbers, $\{n_\ell\}$, which can be used in the following.

The desired location around the train door is then modeled by a potential that forms a double well. Because of the symmetry of the set-up, both sides of the train door are assumed to be equally desirable (this later turns out to be not completely true; see discussion). Furthermore, evidence hints that the distribution is continuous. Hence, a double Gaussian distribution is chosen

$$\begin{aligned} V_\ell(\vec{a}, \vec{b}) = \mu \Bigg(1 - \exp\left[- \left(\frac{\ell_x \Delta x/w - 1/2 - a_1}{b_1} \right)^2 - \left(\frac{\ell_y \Delta x/h - 1/2 + a_2}{b_2} \right)^2 \right] \\ - \exp\left[- \left(\frac{\ell_x \Delta x/w - 1/2 + a_1}{b_1} \right)^2 - \left(\frac{\ell_y \Delta x/h - 1/2 + a_2}{b_2} \right)^2 \right] \Bigg) \end{aligned} \tag{3.1}$$

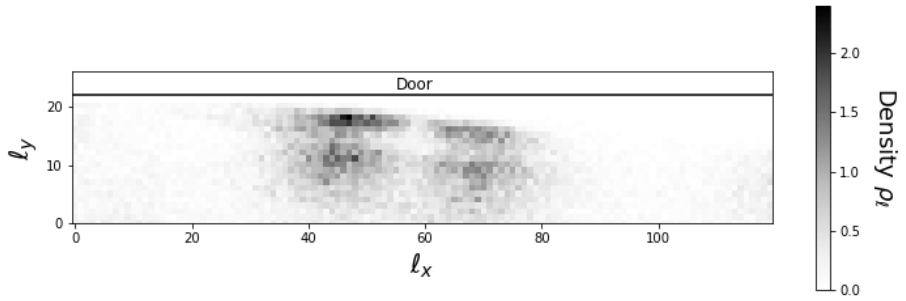

Figure 3.1: Averaged distribution of waiting passengers at the train doors at Eindhoven Central station (NL).

in which $\vec{a}, \vec{b}$ ([-]) are four unknowns representing the separation and width of the distributions respectively and using $\ell = (\ell_x, \ell_y)$ for simplicity. In order to find the site dependent potential parameters, $\vec{a}, \vec{b}$, predictions about the ground state occupation will be made under the assumption that we are in the kinetic free situation ($J \ll 1$). U is fixed to 1, since we have 1 degree of freedom for a specific set of occupation numbers. Then $\mu = U \max_\ell (\rho_\ell)$ is set for the chemical potential, which is related to the maximal occupation, subject to the potential (see 2.34). We find

$$\frac{\mu}{U} = 2.41 \text{ m}^{-2} \tag{3.2}$$

Then, using a multi-dimensional fitting algorithm (Scipy's *curve_fit*) for the distribution in figure 3.1, the values for the parameters can be found.

$$\begin{cases} \vec{a} = \left((98.6 \pm 0.5) \cdot 10^{-3}, (19.4 \pm 0.1) \cdot 10^{-2}\right) \\ \vec{b} = \left((54.6 \pm 0.6) \cdot 10^{-3}, (14.3 \pm 0.2) \cdot 10^{-2}\right) \end{cases}$$

Note that because the values of ℓ_x, ℓ_y span the whole region of interest, these unitless parameters are universal to the problem, regardless of the number of lattice sites. In figure 3.2 the resulting potential is shown.

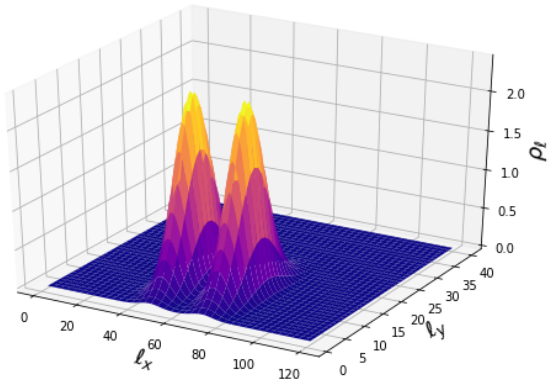

Figure 3.2: Parameter estimation for separation, $\vec{a}$, and width, $\vec{b}$, in the boarding potential using the data in figure 3.1.

3.2 Phase transition

Next, the validity of the idea of a phase transition in the crowd is studied. We believe it is unlikely that multiple lobes in the $(\frac{J}{U}, \frac{\mu - V_\ell}{U})$ phase diagram will be found like in figure 2.3. However, maybe a critical density, ρ_c for fixed J/U, above which passengers freely flow through the crowd, can be identified in analogy with the superfluid phase. For this, a 2D representation of the full platform of Eindhoven central station is studied. We begin by making a distinction between two groups: the stationary group with a speed lower than a certain threshold ($v < 0.1$ m/s) and the dynamical group with speeds larger than this threshold. The dynamical group is passing through the stationary group and our goal is to observe how the density of the dynamical group changes as function of the density of the stationary group. The data of three months in the year 2022 are filtered on our criteria and the densities are calculated and averaged in time for each of the lattice sites of dimensions of 10×10 m^2. It is expected that once the density surpasses the critical density, newly arriving passengers (in the dynamical group) will choose not to remain at the high-density lattice sites and move to neighbouring ones, thus increasing the dynamical density. Indeed such

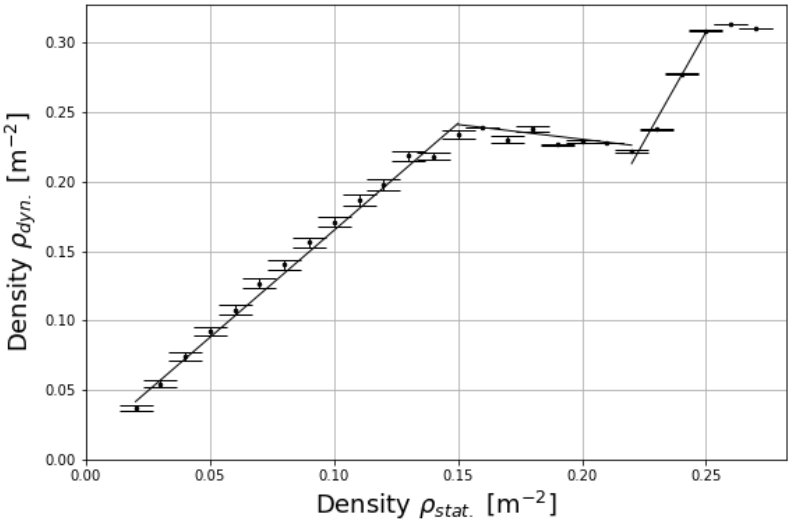

Figure 3.3: Dynamical density, $\rho_{\text{dyn.}}$ against static density, $\rho_{\text{stat.}}$ at Eindhoven central station. Coefficients of the fit can be found in equation 3.5.

a threshold can be observed to some extent, as can be seen in the above figure. We have that first the dynamical density, $\rho_{\text{dyn.}}$, increases somewhat linearly with the static density, $\rho_{\text{stat.}}$. This probably is an effect of the filling of the lattice sites. Once a spot becomes attractive, people both move over it, as well stand still on it. But there is no specific interaction between the two groups. This changes, however, once the density surpasses

$$\rho_p \approx 0.15 \text{ m}^{-2} \tag{3.3}$$

at which a sort of plateau is reached. Here, we believe that the first signs of behaviour is shown that possibly indicates a preferred static - dynamic crowd density balance. One would expect that if the density further increases, the mobility – or dynamical density – decreases due to a mechanism similar to friction. This can be observed, within error, but the trend quickly changes at

$$\rho_c \approx 0.22 \text{ m}^{-2} \tag{3.4}$$

where suddenly the number of people passing the still standing group rises. This is precisely the critical behaviour that was looked for. The different regions in figure 3.3 can be represented by

the relation

$$\rho_{\text{dyn.}}(\rho_{\text{stat.}}) = \begin{cases} (1.54 \pm 0.04)\ \rho_{\text{stat.}} + (0.011 \pm 0.003) & \forall \rho_{\text{stat.}} \in [0, \rho_p) \\ (-0.222 \pm 0.001)\ \rho_{\text{stat.}} + (0.273 \pm 0.0002) & \forall \rho_{\text{stat.}} \in [\rho_p, \rho_c] \\ (3.2 \pm 0.3)\ \rho_{\text{stat.}} + (-0.48 \pm 0.08) & \forall \rho_{\text{stat.}} \in (\rho_c, 0.25] \end{cases} \tag{3.5}$$

which are also plotted in the graph. Considering that increasing the static density, $\rho_{\text{stat.}}$ on the platform corresponds to increasing the chemical potential in the model (since then the lattice can be occupied by more particles, see 2.15), we can relate the two quantities with

$$\frac{\mu_c}{U} = \rho_c \tag{3.6}$$

This chemical potential stands for the filling of the first layer in figure 2.3.

3.3 Modeling the crowd

The last step which is performed, is to make a simulation of the platform during boarding. Since time is now not a physical quantity (as we have removed the "$\hbar$" in the dynamics), the length of the simulation is arbitrary. Thus, the interval of $t \in [0, 1]$ is chosen for convenience. We wish then to incorporate time dynamics by turning on and off the potential with the parameters which we have just derived in 3.3. To make sure that the model predicts a phase transition at the proper density, ρ_c, the train boarding chemical potential and space dependent potential are scaled with the critical potential, μ_c. Then in the model, $g_\ell = 1$ particle will correspond to a density of ρ_c. Define now the time dependent potential as

$$V_\ell(t) = \begin{cases} \mu/\mu_c & \forall t \in [0, 0.25] \cup [0.75, 1] \\ V_\ell(\vec{a}, \vec{b})/\mu_c & \forall t \in [0.25, 0.75] \end{cases} \tag{3.7}$$

The unperturbed Hamiltonian is set to

$$\hat{\mathcal{H}}^0_\ell = -Jz\psi_\ell(\psi_\ell + \hat{b}^\dagger_\ell + \hat{b}_\ell) + U\hat{n}_\ell(\hat{n}_\ell - 1) \tag{3.8}$$

and the perturbation to the Hamiltonian has the form

$$\hat{\mathcal{H}}'_\ell(t) = \begin{cases} 0 & \forall t \in [0, 0.25] \cup [0.75, 1] \\ (V_\ell(\vec{a}, \vec{b}) - \mu)/\mu_c \cdot \hat{n}_\ell & \forall t \in [0.25, 0.75] \end{cases} \tag{3.9}$$

A solution for the unperturbed Hamiltonian is found using the method in 1, yielding both order parameters, $\{\psi_\ell\}$, as well as a set of decoupled wave-functions in occupation number basis, $\{|\phi_\ell\rangle\}$. The formalism described in section 2.7 is then used with the perturbation in equation 3.9 in order to generate time dependent occupation numbers, $\{g_\ell(t)\}$. Then, to obtain again the densities, the occupation numbers are rescaled using $\rho_\ell(t) = \rho_c\ g_\ell(t)$. Note that in the simulation, the parameter for the kinetic energy, J, is not predetermined and can be used to modify the width of the distribution. Then, the last step is to create a movie that shows the evolution of the density in time.

3.4 Conclusion

Some preliminary comparison with the data of train stations in the Netherlands is done and this yielded a model for the boarding process. For this, parameters have been found that signify the dimensions of the distribution of passengers close to the train door, see 3.3. Moreover, a critical density, ρ_c, has successfully been identified, signifying the boundary between a phase in which the flow of people is somewhat constrained as a function of the static density, and a phase in which the newly incoming pedestrians can more easily flow (see equation 3.4). Even though the model already captures some aspects of the density of the crowd (phase transition, dynamics and shape), the predictive power has yet to be tested.

Chapter 4

Discussion

During the process of making the report, a few phenomena stood out that require some reconsideration.

First of all, the term "$\frac{1}{2}$" in 2.15 raises some questions. It might be an artifact of the continuous approach in the derivation (after all, the half can be replaced with any number and 2.17 still holds), but a quantum mechanical reasoning – in which the term shows similarity with the zero-point energy in the quantum harmonic oscillator, $\frac{1}{2}\hbar\omega$ – might be more in place. Moreover, even though hopping has not been involved thus far, interesting enough it does play a role in obtaining the non-zero occupation number. It can numerically be shown that for $J \downarrow 0$ we do find $g_\ell^{(0)} = \frac{1}{2}$ for $\mu = V_\ell$, while for $J = 0$ the occupation truly equals 0. This underlines the importance of a quantum mechanical interpretation of the boson loci, in which the hopping between sites cannot be fully disregarded.

Secondly, the time evolution of the occupation numbers has some ambiguity to it. Since we set $\hbar = 1$, time is not really a physical quantity anymore. Thus, the velocity of transitioning between states is not well defined. This could be changed by studying the typical evolution speed of the train platform and including it in the place of $\hbar$, which is something for future research.

Lastly, a specification for the kinetic energy is purposely not made. This is because of the fact that kinetic energy cannot be easily calculated from the velocity, as every energy quantity is inherently related by the fact that $U = 1$. Thus, a way of finding this quantity respecting the previous requirement should be found.

Bibliography

[1] D. J. Carrascal, J. Ferrer, J. C. Smith, and K. Burke. The Hubbard dimer: A density functional case study of a many-body problem. *Journal of Physics Condensed Matter*, 27(39), 2015. 7

[2] R Celiberto, K L Baluja, and R K Janev. Phase diagram of the Bose-Hubbard Model. 1994. 11

[3] Emiliano Cristiani, Benedetto Piccoli, and Andrea Tosin. *Multiscale modeling of pedestrian dynamics*, volume 12. 2014. 1

[4] Dirk Helbing, Illés Farkas, and Tamás Vicsek. Simulating dynamical features of escape panic. *Nature*, 144(4):297–311, 2000. 1

[5] D. Jaksch. Optical lattices, ultracold atoms and quantum information processing. *Contemporary Physics*, 45(5):367–381, 2004. 7

[6] NS. Reizigersgedrag 2019, 2019. 1

[7] R R Development Core Team. R: A Language and Environment for Statistical Computing. *R Foundation for Statistical Computing*, 1(2.11.1):409, 2011. 10

[8] K. Sheshadri, H. R. Krishnamuethy, R. Pandit, and T. V. Ramakrishnan. Superfluid and insulating phases in an interacting-boson model: Mean-field theory and the rpa. *Epl*, 22(4):257–263, 1993. 6

[9] D. van Oosten, P. van der Straten, and H. T.C. Stoof. Quantum phases in an optical lattice. *Physical Review A. Atomic, Molecular, and Optical Physics*, 63(5):536011–5360112, 2001. 10